One-Step Synthesis of Highly Efficient Nanocatalysts on the Supports with Hierarchical Pores Using Porous Ionic Liquid-Water Gel

Xinchen Kang,[†] Jianling Zhang,[†] Wenting Shang,[†] Tianbin Wu,[†] Peng Zhang,[†] Buxing Han,*,[†] Zhonghua Wu,[‡] Guang Mo,[‡] and Xueqing Xing[‡]

[†]Beijing National Laboratory for Molecular Sciences, Institute of Chemistry, Chinese Academy of Sciences, Beijing 100190, China
[‡]Institute of High Energy Physics, Chinese Academy of Sciences, Beijing 100049, China

Ⓢ *Supporting Information*

ABSTRACT: Stable porous ionic liquid-water gel induced by inorganic salts was created for the first time. The porous gel was used to develop a one-step method to synthesize supported metal nanocatalysts. Au/SiO_2, Ru/SiO_2, $Pd/Cu(2-pymo)_2$ metal−organic framework (Cu-MOF), and Au/polyacrylamide (PAM) were synthesized, in which the supports had hierarchical meso- and macropores, the size of the metal nanocatalysts could be very small (<1 nm), and the size distribution was very narrow even when the metal loading amount was as high as 8 wt %. The catalysts were extremely active, selective, and stable for oxidative esterification of benzyl alcohol to methyl benzoate, benzene hydrogenation to cyclohexane, and oxidation of benzyl alcohol to benzaldehyde because they combined the advantages of the nanocatalysts of small size and hierarchical porosity of the supports. In addition, this method is very simple.

Gels belong to an important class of soft matters.[1] They can be classified into chemical and physical gels. In chemical gels, the cross-linkage results from covalent bonding. In physical gels, the internal 3-D network is cross-linked through weak interactions, such as hydrophobic interactions, hydrogen bonds and crystallite junctions.[2] Gels have wide applications in a variety of fields, including material synthesis,[3] chemical reaction,[4] biomedicine,[5] and organic optoelectronics.[6]

Ionic liquids (ILs) are organic salts which have low melting point (e.g., lower than 100 °C). ILs have many unusual properties, such as negligible vapor pressure, wide liquid range and electrochemical window, good solvents for both organic and inorganic substances, and their properties can be designed by changing the structure of the anion or cation.[7] Applications of ILs in different fields have been studied extensively, such as chemical reaction,[8] extraction and separation,[9] gas absorption,[10] and material synthesis.[11] In recent years, the aggregation behaviors of ILs have been studied widely.[12] ILs can form microemulsions,[13] gels,[2,14] and liquid crystals,[15] etc.

Porous materials have received much interest because of their special structures and applications.[16] Catalysis is the key to enhance the efficiency of many chemical reactions. Heterogeneous catalysts have some obvious advantages, such as easy separation and the possibility of using a fixed-bed reactor. Over the past decades, much effort has been made to design and synthesize efficient heterogeneous catalysts.[17] Porous materials are widely used in the fields of catalysis.[18] The heterogeneous catalysts with hierarchically porous supports are particularly desired in many cases because they integrate the advantages of the pores of different sizes in diffusion and adsorption of the species in the reaction systems.[19] Usually, immobilization of active components on a porous support consists of two steps, preparation of the porous support and immobilization of the active components. There is no doubt that development of one-step protocols to synthesize nanocatalysts immobilized on the supports with hierarchical pores is highly desirable, but is challenging.

In this work, we found that inorganic salts could induce the formation of stable IL-water gel, and the porous gel with hierarchical pores could be easily prepared. The porous gel was used to develop a one-step method to synthesize nanocatalysts immobilized on the supports with hierarchical meso- and macropores. Various metal nanocatalysts of very small size on different supports were synthesized using this new method. The catalysts were very active, selective, and stable for different reactions due to their special structures and morphologies.

Our study by direct observation (Figure S1), conductivity measurement (Figure S2), and small-angle X-ray scattering (SAXS) technique (Figure S3) indicated that the OmimCl (1-octyl-3-methylimidazolium chlorine)-water-$CaCl_2$ and OmimCl-water-$MgCl_2$ systems could form gel at suitable compositions and temperatures, and porous gel could be easily prepared. However, gel could not form without the inorganic salts. That is, the inorganic salts could induce the formation of IL-water gels. The microstructure of the gel obtained from the SAXS study is shown schematically in Figure S4. The detailed results and discussion on the preparation and characterization of the gel and porous gel are given in the Supporting Information (SI, Figures S1−S4, Table S1 and the related discussion). As an example, Figure 1a shows the photograph of the porous gel prepared by stirring the mixture containing 80 wt % IL+20 wt % water with 5 mol % $CaCl_2$ (IL-free basis) at 60 °C, and then cooled down to 25 °C in a water bath. The photograph of the gel prepared with the same amounts of components is shown in Figure 1b. As expected, the volume of the porous gel was much larger than that of the gel and was not transparent because of the existence of the air bubbles (pores). The confocal laser scanning microscopy (CLSM) images of the
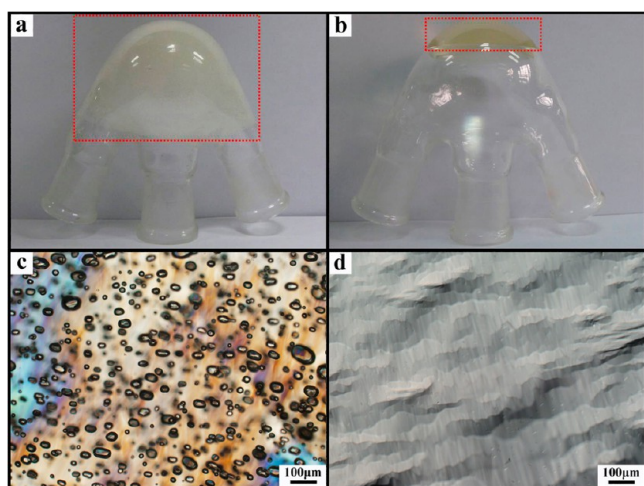
Figure 1. The photographs of the porous gel (a) and gel (b), and the CLSM images of the porous gel (c) and gel (d).

porous gel and gel are shown in Figure 1, panels c and d, respectively. It can be seen clearly that there were numerous pores in the porous gel. We emphasize that only the larger pores in the porous gel could be observed due to the resolution limitation of CLSM technique. Our study indicated that the gel and porous gel were stable at least for two months at room temperature.

The gels created in this work can find wide applications. As an example of its utilization, we developed a one-step method to prepare metal nanocatalysts immobilized on the supports with hierarchical pores, and Au/SiO_2, Ru/SiO_2, $Pd/Cu(2-pymo)_2$ metal−organic framework (Cu-MOF), and Au/polyacrylamide (PAM) were synthesized. The route to synthesize the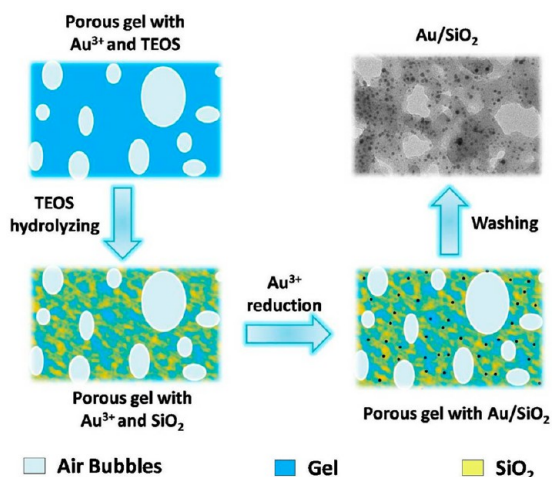 catalysts is shown schematically in Figure 2, taking the synthesis of Au/SiO_2 as an example. The detailed procedures for the preparation of each of these catalysts are described in the SI. Briefly, the IL-water-$CaCl_2$ porous gel with $HAuCl_4$ and Si precursor tetraethoxysilane (TEOS) was prepared. Porous SiO_2 was formed in the porous gel by hydrolysis of the TEOS. The gel was destroyed after mixing with $NaBH_4$ aqueous solution because it was not stable at higher water content, as seen from the results in Table S1. At the same time, the Au^{3+} in the porous SiO_2 was reduced by the

Figure 2. The route for the synthesis of the Au/SiO_2 catalysts.

$NaBH_4$, and Au/SiO_2 catalyst was obtained after removing the IL and water by washing with solvents and drying.

The SEM image of the Au/SiO_2 catalyst with 6 wt % Au is shown in Figure 3a. Figure 3b−f presents the TEM images of
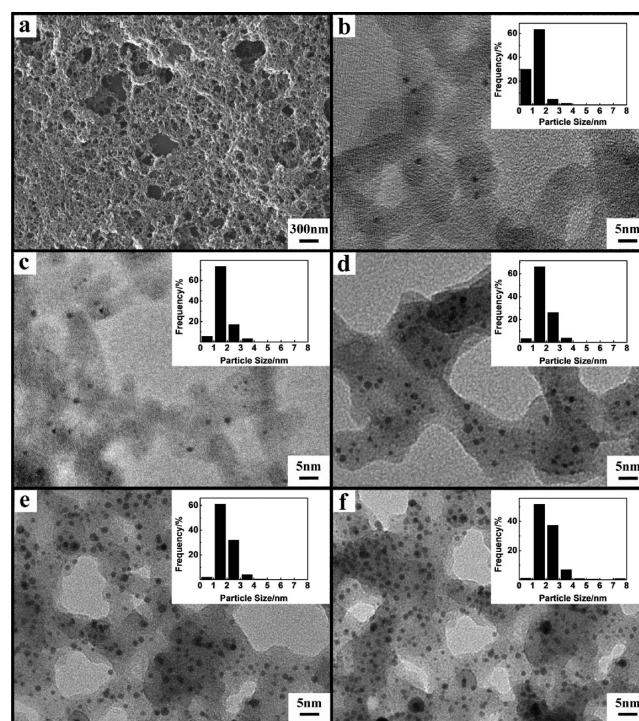

Figure 3. SEM and TEM images of the Au/SiO_2 composites: (a) SEM image with 6.0 wt % Au; TEM images with (b) 1.0, (c) 2.0, (d) 4.1, (e) 6.0, and (f) 8.1 wt % Au. The insets in (b−f) show the size distribution of Au particles.

the Au/SiO_2 catalysts with different Au loadings, and the average size of Au in the composites are provided in Table 1.

Table 1. Catalytic Performances of the Au/SiO_2 Composites for Oxidative Esterification of Benzyl Alcohol to Methyl Benzoate[a]

entry	Au loading [wt %][b]	average size [nm]	t [h][c]	C [%][c]	S [%][c]
1	1.0	1.5	24.0	>99	>99
2	2.0	1.7	14.0	>99	>99
3	4.1	1.9	7.0	>99	>99
4	6.0	2.0	4.0	>99	>99
5	8.1	2.1	5.5	>99	>99

[a]Reaction conditions: 5 μmol of Au, 1 mmol of benzyl alcohol, 2 mL of methanol, 0.5 mmol of K_2CO_3, 0.5 MPa O_2, 50 °C. [b]The loading amounts of Au were determined by ICP-AES (VISTA-MPX). [c]t = Reaction time, C = Conversion, S = Selectivity.

All the Au loadings in the catalysts were determined by ICP-AES (VISTA-MPX), which agreed well with the calculated Au loadings on the basis of the Au and Si precursors used. All the images showed that the SiO_2 supports had hierarchical pores. The porosity of the SiO_2 support and Au/SiO_2 catalysts was further characterized by N_2 adsorption/desorption method (Figure S5). The BET surface area, total pore volume, and

3769

dx.doi.org/10.1021/ja5001517 | *J. Am. Chem. Soc.* 2014, 136, 3768−3771

average pore diameter are shown in Table S2. The pore volumes of Au/SiO$_2$ catalysts were smaller than those of the SiO$_2$ support, suggesting that the Au nanoparticles were deposited on the walls of the pores. The generation of the catalyst, in which the metal nanocatalysts of small size and narrow size distribution were immobilized on the support with hierarchical pores, is easy to understand considering the special properties and morphologies of the porous gel. The air bubbles in the porous gel were responsible for the pores of the SiO$_2$ formed by the hydrolysis of TEOS. The IL-water gel domains with Au^{3+} ions were trapped in the SiO$_2$ frame as shown in Figure 2. Au nanoparticles were generated after the Au^{3+} ions were reduced. The spaces occupied by the IL-water domains became pores of the support after the IL and water were removed. The air bubbles and the IL-water gel domains acted as the templates for the formation the pores of the support in the final catalyst. Au nanoparticles were formed in situ in the pores, which was favorable to forming small Au particles. Therefore, the Au nanoparticles of small size and narrow size distribution were immobilized uniformly on the porous support. As expected, the size of the supported Au particles increased slightly with the increase of the loading amount in the catalysts. However, the size of the Au particles was still very small even when the Au loading was as high as 8 wt %, which is another advantage of this method.

The TEM images of the Ru/SiO$_2$, Pd/Cu-MOF, and Au/PAM catalysts are shown in Figure S6. The Pd/Cu-MOF was further characterized by wide-angle powder X-ray diffraction (XRD, Figure S7), thermogravimetric Analysis (TGA, Figure S8) and ICP-AES (VISTA-MPX), which confirms that the MOF was Cu(2-pymo)$_2$.[20] Similarly, the metal nanocatalysts of very small size with narrow size distribution were immobilized on the supports with hierarchical pores. The average size of Au and Ru were further characterized by XRD technique (Figure S9). The size of the Ru nanoparticles in Ru/SiO$_2$ with 5 wt % Ru calculated by Scherrer Equation was 0.89 nm, which is very difficult to fabricate by other methods. The result is consistent with that obtained by TEM method (Figure S6b). The supports can be inorganic, inorganic–organic hybrid and organic polymer, indicating that the method proposed in this work is versatile for preparing the metal nanocatalysts immobilized on the supports with hierarchical pores.

Esterification of benzyl alcohol to methyl benzoate,[21] benzene hydrogenation to cyclohexane,[22] and oxidation of benzyl alcohol to benzaldehyde[23] are important reactions. The catalytic performances of the catalysts prepared for different reactions were studied. The results for the oxidative esterification of benzyl alcohol to methyl benzoate catalyzed by the Au/SiO$_2$ are listed in Table 1. The reaction proceeded smoothly under mild condition. The activity and selectivity of all the catalysts with different Au loadings were very high. The activity of the catalysts increased with the increase of Au loading at first and then decreased, and reached highest at the Au loading of 6.0 wt %. The Ru/SiO$_2$ catalysts were used to promote benzene hydrogenation to cyclohexane (Table 2). Similarly, the catalyst with higher Ru loading exhibited higher activity. The conversion and selectivity for the solvent-free oxidation of benzyl alcohol to benzaldehyde was conducted using the Pd/Cu-MOF as the catalyst. The dependence of conversion and selectivity on reaction time is shown in Figure 4. The catalyst had very high activity and selectivity even at ambient pressure. The TOF values of the catalytic reactions are compared with the typical results reported in the literature

Table 2. Catalytic Performance of the Ru/SiO$_2$ Catalyst for Benzene Hydrogenation to Cyclohexane[a]

$$\text{(benzene)} + H_2 \xrightarrow{\text{Ru/SiO}_2} \text{(cyclohexane)}$$

entry	Ru loading [wt %]	T [°C]	t [h]	Y [%][b]	TOF[c]
1	1.0	100	1.5	>99	1667
2	1.0	50	4.5	>99	556
3	5.0	100	0.5	>99	5000
4	5.0	50	3.0	>99	833

[a]Reaction conditions: 10 μmol of Ru, 25 mmol benzyl, 2 MPa H$_2$. [b]Yield of cyclohexane. [c]TOF (turnover frequency) was calculated as conversion of moles of benzene per mol of Ru per hour.
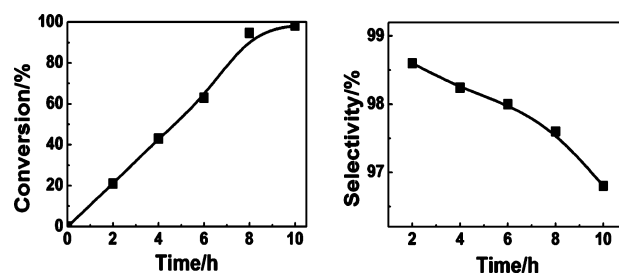

Figure 4. The conversion and selectivity of solvent-free oxidation of benzyl alcohol to benzaldehyde. Reaction conditions: 0.1 mol benzyl alcohol and 1 μmol Pd catalyst, 1 atm O$_2$ at 100 °C.

(Table S3). Obviously, the catalysts prepared in our work are much more active mainly because they combined the advantages of the nanocatalysts of small size and hierarchical porosity of the supports. The stability and reusability of the Au/SiO$_2$ catalyst with 6.0 wt % Au (entry 4 of Table 1) was studied, and the results are shown in Figure S10. The conversion and selectivity of the catalyst did not decrease noticeably after reused five times, indicating that the catalysts were very stable.

There are at least two reasons for the excellent catalytic performances of the catalysts for all the studied reactions. First, the size of the metal nanoparticles was very small and the size distribution was narrow. Second, the hierarchical porosity of the supports was favorable to both adsorption of the reactants and mass transfer of the species. The metal nanocatalysts existed mainly in the pores of the supports, which made the catalysts very stable.

In summary, we have created porous IL-H$_2$O-inorganic salt gels. A one-step protocol to synthesize metal nanocatalysts of controlled size on supports with hierarchical porosity has been proposed using the special nature of the porous gel, and different heterogeneous catalysts have been designed and fabricated. The supports range from inorganic, inorganic–organic hybrid, to organic materials. The catalysts prepared have very high activity, selectivity, and stability for different reactions because they integrate the advantages of the nanocatalysts of very small size and the supports with hierarchical pores. We believe that the new and simple route has wide applications in the synthesis of various highly efficient heterogeneous catalysts.

■ ASSOCIATED CONTENT

Ⓢ Supporting Information

Experimental section; the detailed results and discussion on the gel and porous gel; supporting figures, tables and references.

This material is available free of charge via the Internet at http://pubs.acs.org.

■ AUTHOR INFORMATION

Corresponding Author

hanbx@iccas.ac.cn

Notes

The authors declare no competing financial interest.

■ REFERENCES

(1) (a) Steed, J. W. *Chem. Soc. Rev.* **2010**, *39*, 3686−3699. (b) Piepenbrock, M. O. M.; Lloyd, G. O.; Clarke, N.; Steed, J. W. *Chem. Rev.* **2010**, *110*, 1960−2004.

(2) Le Bideau, J.; Viau, L.; Vioux, A. *Chem. Soc. Rev.* **2011**, *40*, 907−925.

(3) Subban, C. V.; Zhou, Q.; Hu, A.; Moylan, T. E.; Wagner, F. T.; DiSalvo, F. J. *J. Am. Chem. Soc.* **2010**, *132*, 17531−17536.

(4) Miravet, J. F.; Escuder, B. *Tetrahedron* **2007**, *63*, 7321−7325.

(5) Jayawarna, V.; Ali, M.; Jowitt, T. A.; Miller, A. F.; Saiani, A.; Gough, J. E.; Ulijn, R. V. *Adv. Mater.* **2006**, *18*, 611−614.

(6) Kitahara, T.; Shirakawa, M.; Kawano, S.; Beginn, U.; Fujita, N.; Shinkai, S. *J. Am. Chem. Soc.* **2005**, *127*, 14980−14981.

(7) (a) Swatloski, R. P.; Spear, S. K.; Holbrey, J. D.; Rogers, R. D. *J. Am. Chem. Soc.* **2002**, *124*, 4974−4975. (b) Rogers, R. D.; Seddon, K. R. *Science* **2003**, *302*, 792−793. (c) Wasserscheid, P.; Welton, T. *Ionic Liquids in Synthesis*; Wiley-VCH: Weinheim, 2008. (d) Dupont, J. *Acc. Chem. Res.* **2011**, *44*, 1223−1231. (e) Lin, Y. H.; Zhao, A. D.; Tao, Y.; Ren, J. S.; Qu, X. G. *J. Am. Chem. Soc.* **2013**, *135*, 4207−4210.

(8) (a) Hallett, J. P.; Welton, T. *Chem. Rev.* **2011**, *111*, 3508−3576. (b) Allen, C.; Sambasivarao, S. V.; Acevedo, O. *J. Am. Chem. Soc.* **2013**, *135*, 1065−1072.

(9) (a) Blanchard, L. A.; Hancu, D.; Beckman, E. J.; Brennecke, J. F. *Nature* **1999**, *399*, 28−29. (b) Bara, J. E.; Camper, D. E.; Gin, D. L.; Noble, R. D. *Acc. Chem. Res.* **2010**, *43*, 152−159.

(10) (a) Gurkan, B. E.; de la Fuente, J. C.; Mindrup, E. M.; Ficke, L. E.; Goodrich, B. F.; Price, E. A.; Schneider, W. F.; Brennecke, J. F. *J. Am. Chem. Soc.* **2010**, *132*, 2116−2117. (b) Wang, C. M.; Cui, G. K.; Luo, X. Y.; Xu, Y. J.; Li, H. R.; Dai, S. *J. Am. Chem. Soc.* **2011**, *133*, 11916−11919.

(11) (a) Lee, J. S.; Wang, X. Q.; Luo, H. M.; Baker, G. A.; Dai, S. *J. Am. Chem. Soc.* **2009**, *131*, 4596−4597. (b) Fechler, N.; Fellinger, T. P.; Antonietti, M. *Adv. Mater.* **2013**, *25*, 75−79.

(12) (a) Greaves, T. L.; Drummond, C. J. *Chem. Soc. Rev.* **2013**, *42*, 1096−1120. (b) Zhang, J. L.; Han, B. X. *Acc. Chem. Res.* **2013**, *46*, 425−433.

(13) (a) Gao, H. X.; Li, J. C.; Han, B. X.; Chen, W. N.; Zhang, J. L.; Zhang, R.; Yan, D. D. *Phys. Chem. Chem. Phys.* **2004**, *6*, 2914−2916. (b) Eastoe, J.; Gold, S.; Rogers, S. E.; Paul, A.; Welton, T.; Heenan, R. K.; Grillo, I. *J. Am. Chem. Soc.* **2005**, *127*, 7302−7303.

(14) (a) Firestone, M. A.; Dzielawa, J. A.; Zapol, P.; Curtiss, L. A.; Seifert, S.; Dietz, M. L. *Langmuir* **2002**, *18*, 7258−7260. (b) Jiang, W. Q.; Hao, J. C.; Wu, Z. H. *Langmuir* **2008**, *24*, 3150−3156. (c) Gu, Y. Y.; Zhang, S. P.; Martinetti, L.; Lee, K. H.; McIntosh, L. D.; Frisbie, C. D.; Lodge, T. P. *J. Am. Chem. Soc.* **2013**, *135*, 9652−9655.

(15) (a) Gao, Y. A.; Slattery, J. M.; Bruce, D. W. *New. J. Chem.* **2011**, *35*, 2910−2918. (b) Fong, C.; Le, T.; Drummond, C. J. *Chem. Soc. Rev.* **2012**, *41*, 1297−1322.

(16) (a) Shah, P. S.; Sigman, M. B.; Stowell, C. A.; Lim, K. T.; Johnston, K. P.; Korgel, B. A. *Adv. Mater.* **2003**, *15*, 971−974. (b) Cooper, A. I. *Angew. Chem., Int. Ed.* **2012**, *51*, 7892−7894. (c) Yue, Y. F.; Qiao, Z. A.; Fulvio, P. F.; Binder, A. J.; Tian, C. C.; Chen, J. H.;

Nelson, K. M.; Zhu, X.; Dai, S. *J. Am. Chem. Soc.* **2013**, *135*, 9572−9575.

(17) (a) Corma, A. *Chem. Rev.* **1997**, *97*, 2373−2419. (b) Zheng, N. F.; Stucky, G. D. *J. Am. Chem. Soc.* **2006**, *128*, 14278−14280. (c) Xiao, C. X.; Wang, L. L.; Maligal-Ganesh, R. V.; Smetana, V.; Walen, H.; Thiel, P. A.; Miller, G. J.; Johnson, D. D.; Huang, W. Y. *J. Am. Chem. Soc.* **2013**, *135*, 9592−9595.

(18) (a) Kopilevich, S.; Gil, A.; Garcia-Ratés, M.; Bonet-Ávalos, J.; Bo, C.; Müller, A.; Weinstock, I. A. *J. Am. Chem. Soc.* **2012**, *134*, 13082−13088. (b) Totten, R. K.; Kim, Y. S.; Weston, M. H.; Farha, O. K.; Hupp, J. T.; Nguyen, S. T. *J. Am. Chem. Soc.* **2013**, *135*, 11720−11723.

(19) (a) Côté, A. P.; Benin, A. I.; Ockwig, N. W.; O'Keeffe, M.; Matzger, A. J.; Yaghi, O. M. *Science* **2005**, *310*, 1166−1170. (b) Hasegawa, S.; Horike, S.; Matsuda, R.; Furukawa, S.; Mochizuki, K.; Kinoshita, Y.; Kitagawa, S. *J. Am. Chem. Soc.* **2007**, *129*, 2607−2614. (c) Zhang, Y. G.; Riduan, S. N. *Chem. Soc. Rev.* **2012**, *41*, 2083−2094.

(20) Tabares, L. C.; Navarro, J. A. R.; Salas, J. M. *J. Am. Chem. Soc.* **2001**, *123*, 383−387.

(21) (a) Oliveira, R. L.; Kiyohara, P. K.; Rossi, L. M. *Green Chem.* **2009**, *11*, 1366−1370. (b) Jagadeesh, R. V.; Junge, H.; Pohl, M. M.; Radnik, J.; Brückner, A.; Beller, M. *J. Am. Chem. Soc.* **2013**, *135*, 10776−10782.

(22) Miao, S. D.; Liu, Z. M.; Han, B. X.; Huang, J.; Sun, Z. Y.; Zhang, J. L.; Jiang, T. *Angew. Chem., Int. Ed.* **2006**, *45*, 266−269.

(23) Enache, D. I.; Edwards, J. K.; Landon, P.; Solsona-Espriu, B.; Carley, A. F.; Herzing, A. A.; Watanabe, M.; Kiely, C. J.; Knight, D. W.; Hutchings, G. J. *Science* **2006**, *311*, 362−365.